Sphingomyelinase Induces Lipid Microdomain Formation in a Fluid Phosphatidylcholine/Sphingomyelin Membrane†

Juha M. Holopainen, Marappan Subramanian, and Paavo K. J. Kinnunen*

Helsinki Biophysics and Biomembrane Group, Department of Medical Chemistry, Institute of Biomedicine, University of Helsinki, Finland

Received April 22, 1998; Revised Manuscript Received August 26, 1998

ABSTRACT: The behaviors of two chemically well-defined sphingolipids, *N*-palmitoyl-sphingomyelin (C16:0-SM) and the corresponding ceramide (C16:0-Cer), in a 1-palmitoyl-2-oleoyl-*sn*-glycero-3-phosphatidylcholine (POPC) matrix were compared. Minor attenuation of lateral diffusion upon increasing the mole fraction of C16:0-SM (X_{SM}, up to 0.25) was indicated by the slight decrement in the excimer/monomer intensity ratio (I_e/I_m) for a trace amount (mole fraction $X = 0.01$) of a pyrene-labeled ceramide analogue (*N*-[(pyren)-1-yl]decanoyl-sphingosine, PDCer) in keeping with the miscibility of C16:0-SM in POPC. Increasing membrane order was revealed by the augmented polarization *P* for diphenylhexatriene (DPH). In contrast, when C16:0-Cer was substituted for C16:0-SM an approximately 1.6-fold increase in I_e/I_m for PDCer was evident upon increasing X_{cer}, with parallel increment in DPH polarization. In agreement with our recent data on natural ceramides in dimyristoylphosphatidylcholine (DMPC) bilayers [Holopainen et al. (1997) *Chem. Phys. Lipids 88*, 1−13], we conclude that C16:0-Cer becomes enriched into microdomains in the fluid POPC membrane. Interestingly, enhanced formation of microdomains by ceramide was observed when the total sphingolipid content in tertiary alloys with POPC was maintained constant ($X_{cer} + X_{SM} = 0.25$) and the SM/Cer stoichiometry was varied. Finally, when ceramide was generated enzymatically in POPC/C16:0-SM (3:1, molar fraction) LUVs by sphingomyelinase (SMase, *Bacillus cereus*), maximally approximately 85% of hydrolysis of sphingomyelin was measured within <3 min at 30 °C. The formation of ceramide was accompanied by a closely parallel increase in DPH polarization. There was also an increase in I_e/I_m for PDCer; however, these changes in I_e/I_m were significantly slower, requiring ≈105 min to reach a steady state. These data show that the rapid enzymatic formation of ceramide under these conditions is followed by much slower reorganization process, resulting in the formation of microdomains enriched in this lipid.

Ceramide has been recently confirmed to function as a second messenger in several cellular processes, including apoptosis, growth suppression, differentiation, and cell senescence (for recent reviews, see refs *1*−*7*). A signaling pathway involving MAP kinase has been proposed (*8, 9*). Although several downstream targets for ceramide have been suggested, only protein kinase C-ξ, phospholipase A_2, and CAPP (ceramide-activated protein phosphatase) have so far been demonstrated to be activated by this lipid in vitro (for a review, see ref *10*). In addition to its role in cell signaling, ceramide has been suggested to mediate the aggregation of plasma low-density lipoproteins and thus enhance the formation of atherosclerotic plagues (*11*). Ceramides are found ubiquitously in stratum corneum of the skin (*12*) where they are assumed to be responsible for retaining normal skin function such as its impermeability (*13*). Disturbances in sphingolipid metabolism are known to underlie several dermatological disorders (*14*).

In cellular membranes ceramide is formed upon the hydrolytic removal of the phosphocholine moiety of sphingomyelin by sphingomyelinase (SMase[1]) (*2, 15*). Several sphingomyelinase species, presumably serving distinct functions, have been identified in eukaryotic cells (*15*). Notably, bacterial SMases function as toxins damaging their host cell membrane (*16*). Subjecting cells to the action of externally added SMase has been shown to cause apoptosis (*9*). The eukaryote SMases are activated after the binding of extracellular ligands such as calcitriol, tumor necrosis factor α, γ-interferon, and interleukin-1 to their receptors in the plasma membrane (ref *9* and references therein). The sphingomyelin

† This study was supported by the Finnish State Medical Research Council and Biocentrum Helsinki. J.M.H. is supported by the M.D./Ph.D. program of the University of Helsinki and the Finnish Medical Foundation.

* To whom correspondence should be addressed: Institute of Biomedicine, Department of Medical Chemistry, P.O. Box 8 (Siltavuorenpenger 10A), FIN-00014, University of Helsinki, Finland. E-mail: Paavo.Kinnunen@Helsinki.Fi. Fax: 358-9-1918276. Tel: 358-9-1918237.

[1] Abbreviations: bisPDPC, 1,2-bis[(pyren)-1-yl]decanoyl-*sn*-glycero-3-phosphocholine; C16:0-Cer, *N*- palmitoyl-sphingosine; DCC, dicyclohexylcarbodiimide; DMPC, 1,2-dimyristoyl-*sn*-glycero-3-phosphocholine; DPH, 1,6-diphenyl-1,3,5-hexatriene; DPPC, 1,2-dipalmitoyl-*sn*-glycero-3-phosphocholine; I_e, excimer fluorescence intensity at 470 nm; I_m, monomer fluorescence intensity at 380 nm; LUVs, large unilamellar vesicles; POPC, 1-palmitoyl-2-oleoyl- sn-glycero-3-phosphocholine; C16:0-SM, *N*-palmitoyl-sphingomyelin; *P*, fluorescence polarization; PPDPC, 1-palmitoyl-2-[(pyren)-1-yl]decanoyl-*sn*-glycero-3-phosphocholine; PDCer, *N*-[(pyren)-1-yl]decanoyl-sphingosine; SM, sphingomyelin; SMase, sphingomyelinase; THF, tetrahydrofuran; τ, fluorescence lifetime.

10.1021/bi980915e CCC: $15.00
Published on Web 11/20/1998

cycle is terminated with the transfer of phosphocholine from phosphatidylcholine to ceramide, so as to regenerate sphingomyelin. The production of ceramide has been suggested to be localized in caveolae, specific plasma membrane invaginations having a diameter of 50−100 nm, and enriched in this lipid (*17*). A possible role for these detergent insoluble domains in signal transduction has been suggested (*18*). Binding of interleukin-1β (IL-1β) to caveolae-resembling sphingomyelin-rich plasma membrane regions causes an increment in diacylglycerol concentration and hydrolysis of sphingomyelin to ceramide (*17*). The contents of ceramide in the membranes of cells undergoing apoptosis have been measured to reach 10 mol % of the total phospholipid (*3*). Similar content of natural ceramides was required for the formation of microdomains enriched in this lipid in vitro (*19*).

The precursor for ceramide, sphingomyelin (SM), is found in relatively large amounts in many cellular membranes, and in plasma membrane it is mainly present in the outer monolayer. The physicochemical properties and thermal phase behavior of SM have been subjects of a number of studies. SMs have rather high melting temperatures, 40.5−41 °C for C16:0-SM (*20, 21*) and 30−40 °C for the species isolated from bovine brain (*22*). Both egg yolk SM and C16:0-SM have been shown to be completely miscible in gel state as well as liquid-crystalline dimyristoylphosphatidylcholine (DMPC) (*20, 23*). Besides having a structural role, SM seems to be also involved in several cellular processes. SM and also other sphingolipids are required for fusion of the Semliki forest virus to host cells (*24*). In a mutant melanocyte cell line, hydrolysis of sphingomyelin resulted in the detachment of cells from the substratum (*25*). A defect in SM metabolism leads to Niemann-Pick disease, and SM has also been linked to cancer (*26*).

In contrast to SM, only a few studies on the physicochemical properties of ceramide attempting to relate to its cellular effects have been accomplished. The thermotropic behavior of nonhydroxy and α-hydroxy fatty acid ceramides has been resolved by differential scanning calorimetry and X-ray diffraction (*27, 28*). Ceramide has been suggested to cause defects in DPPC bilayers and thus activate PLA_2 (*29*). Formation of ceramides by sphingomyelinase has been shown to cause aggregation and/or fusion of LUVs in vitro (*30, 31*). Our previous studies on natural ceramide in DMPC LUVs (*19*) using differential scanning calorimetry and fluorescence spectroscopy provided evidence for ceramide-enriched microdomains in both gel states as well as fluid bilayers of DMPC. This process is of interest as there is ample evidence showing biological membranes to be organized into functionally distinct domains (for reviews, see refs *32, 33*). The above study was carried out with natural bovine ceramide, which is highly heterogeneous in its fatty acid composition. In the present work these data were substantiated using a chemically well-defined synthetic ceramide (C16:0-Cer) in an unsaturated phospholipid, POPC matrix. Moreover, we could also show that the enzymatic generation of ceramide from sphingomyelin induces microdomain formation in these LUVs. However, while the hydrolytic reaction could be rapidly (<3 min) driven to completion, the reorganization of the product into microdomains within the bilayer required considerably longer time (>100 min, at 30 °C).

EXPERIMENTAL PROCEDURES

Materials. Hepes, EDTA, *N*-hydroxy succinimide, D-sphingosine, and POPC were from Sigma, and dicyclohexylcarbodiimide (DCC) was from Fluka (Buchs, Switzerland). C16:0-ceramide and C16:0-sphingomyelin were from Northern Lipids Inc. (Vancouver, British Columbia, Canada) and bisPDPC and [(pyren)-1-yl]decanoic acid from K&V Bioware (Espoo, Finland). [*N*-Methyl-^{14}C]sphingomyelin (specific activity 2.07 GBq/mmol) was obtained from Amersham Life Science (Buckinghamshire, UK) and dipalmitoylphosphatidylcholine (DPPC) from Coatsome (Amagasaki, Hyogo, Japan). $CaCl_2$ dihydrate and $MgCl_2$ hexahydrate were from Merck (Darmstadt, Germany). The purity of the above lipids was checked by thin-layer chromatography on silicic acid-coated plates (Merck, Darmstadt, Germany) using chloroform/methanol/water (65:25:4, v/v/v) for the phospholipids and C16:0-sphingomyelin and 1,2-dichloroethane/methanol/water (90:20:0.5, v/v/v) as solvent systems for the ceramides. Examination of the plates after iodine staining, or when appropriate by fluorescence illumination, revealed no impurities. The concentrations of the pyrene-labeled ceramide (see below) and bisPDPC were determined spectrophotometrically using 42 000 and 84 000 cm^{-1} at 342 nm as the respective molar extinction coefficients. Concentrations of the other lipids were determined gravimetrically using a high-precision electrobalance (Cahn, Cerritos, CA). Sphingomyelinase (*Bacillus cereus*, from Sigma) was stored at −20 °C in 100 μL aliquots in plastic vials at a concentration of 10 units/mL in distilled water. The specific activity of this enzyme preparation was 100−300 units/mg of protein, with one unit defined as the hydrolysis of one micromole of SM per minute at pH 7.4 at 37 °C. Pro analysis grade solvents were from Merck (Darmstadt, Germany).

Synthesis of the Pyrene-Labeled Ceramide Analogue, PDCer. Pyrenedecanoic acid was converted into its succinimide ester by reacting with *N*-hydroxy succinimide in the presence of DCC in dry chloroform (*34*). More specifically, DCC (0.7 g, 3.3 mmol) was added to a solution of pyrenedecanoic acid (1.16 g, 3 mmol) and *N*-hydroxysuccinimide (0.345 g, 3 mmol) dissolved in dry chloroform (80 mL). The reaction mixture was then stirred for 12 h at room temperature. The separated solid dicyclohexylurea was filtered and rinsed with chloroform to extract the product. Solvents were removed under reduced pressure using a rotatory evaporator to yield a white crystalline solid (1.26 g, 90% yield) which appeared as a single spot upon thin-layer chromatography on silicic acid-coated plates developed with chloroform/methanol (7:3, v/v). Recrystallization from ethanol yielded 1.2 g (87%) of pure *N*-hydroxysuccinimide ester of pyrenedecanoic acid (mp 100−102 °C). *N*-pyrenedecanoyl-D-sphingosine (PDCer) was then synthesized by condensation of D-sphingosine with *N*-hydroxysuccinimide ester of pyrenedecanoic acid as described previously (*35*). In brief, D-sphingosine (15 mg, 50 μmol, dissolved in 3.0 mL of freshly distilled tetrahydrofuran, THF, dried over metallic sodium) was added to a solution of succinimide ester of pyrenedecanoic acid (23.5 mg, 50 μmol) in 3.0 mL of THF in a stoppered test tube. The reaction mixture was then left overnight at room temperature, with gentle stirring. The solution was subsequently dried under a stream of nitrogen to approximately half of the volume and sufficient water

added to induce crystallization of the reaction product. White crystalline PDCer (27.8 mg, 85% yield) separated out and was filtered and dried. Recrystallization from methanol/water mixture (1:1, v/v) gave pure product (80% yield, mp 83−85 °C), revealing a single spot upon thin-layer chromatography performed as above.

Liposome Preparation. Appropriate amounts of the lipid stock solutions were mixed in chloroform to obtain the desired compositions with either bisPDPC (mole fraction $X = 0.001$), PDCer ($X = 0.01$), or DPH ($X = 0.002$) included as fluorescent probes. The resulting mixtures were then evaporated to dryness under a stream of nitrogen and traces of solvent subsequently removed by evacuating under reduced pressure for at least 12 h. If the dry residue was not used immediately, it was stored at −20 °C. The lipid residues were hydrated at 50 °C in 5 mM Hepes, 0.1 mM EDTA, pH 7.4, to yield a lipid concentration of 0.375 or 0.75 mM and maintained at this temperature for 30 min prior to irradiation for 2 min in a bath-type ultrasonicator (NEY Ultrasonik 104H, Yucaipa, CA). The resulting dispersions were subsequently processed to larger unilamellar vesicles (LUVs) by extrusion through a stack of two Millipore (Bedford, MA) 0.1 mm pore size polycarbonate filters using a Liposofast-Pneumatic (Avestin, Ottawa, Canada), essentially as described by MacDonald et al. (*36*). Importantly, the pressure used for the extrusion of POPC vesicles through the stack of polycarbonate membranes was 10 psi (≈69 kPa). This pressure was also sufficient for the extrusion of POPC vesicles containing either SM at $X = 0.25$ or C16:0-Cer at $X = 0.025$. However, for POPC MLVs containing both SM and Cer (e.g., $X_{SM} = 0.225$ and $X_{cer} = 0.025$), a significantly higher pressure of approximately 12.5 psi (≈88 kPa) was necessary.

Measurement of I_e/I_m. A monomeric excited-state pyrene may relax to ground state by emitting photons with a maximum wavelength at ≈380 nm (I_m), the exact peak energy and spectral fine structure depending on solvent polarity. During its lifetime, the excited-state pyrene may also form a characteristic short-lived complex, excimer (excited dimer) with a ground-state pyrene. This complex relaxes back to two ground-state pyrenes by emitting quanta as a broad and featureless band centered at ≈480 nm (I_e). In the absence of possible quantum mechanical effects (*37*) and the formation of superlattices, the excimer to monomer fluorescence intensity ratio (I_e/I_m) is proportional to the rate of collisions between the pyrenes. Consequently, for a single pyrene moiety containing lipid analogue such as PDCer, the value for I_e/I_m reflects the lateral mobility as well as the local concentration of the fluorophore in the membrane (for recent reviews, see refs *38*, *39*). Fluorescence emission spectra for LUVs labeled with the different pyrene probes were recorded with a Perkin-Elmer LS50B spectrofluorometer equipped with a magnetically stirred, thermostated cuvette compartment. The excitation wavelength was 344 nm and the excitation and emission bandwidths were 4 nm for PDCer and 7.5 nm for bisPDPC, respectively. Two milliliters of liposome solution (45 nmol of lipid) in a four-window quartz cuvette were used in each measurement with temperature maintained at 30 °C. Each sample was equilibrated for 2 min before recording the spectrum. Three scans were averaged, and the emission intensities at ≈380 and 470 nm were taken for I_m and I_e, respectively. As only relative values were of interest, the measured spectra were not corrected for instrument response.

Fluorescence Polarization and Lifetime Measurements. DPH was included into liposomes to yield a lipid/DPH molar ratio of approximately 500:1. Polarized emission was measured in the L-format using polaroid film-type prisms in the Perkin-Elmer LS50B spectrofluorometer. Excitation at 360 nm and emission at 450 nm were selected with monochromators and using 5 nm bandwidths. The samples were maintained in the cuvette for 2 min prior to the measurement of polarization, averaging the signal over a 5 s interval. Values of steady-state fluorescence polarization P were calculated using routines of the software provided by Perkin-Elmer and data analyzed using Microsoft Excel.

Fluorescence lifetimes were measured using a commercial laser spectroscopy system (PTI, Ontario, Canada). A train of 500 ps excitation pulses (at 340 nm and at a repetition rate of 10 Hz) from a nitrogen laser were used to pump a dye (rhodamine 6G) laser. Pulses from the latter were channeled to a frequency doubler. Emission decays for DPH at 450 nm were detected by a photomultiplier tube. The average of three subsequent decay curves was used to calculate τ. The instrument response functions were measured separately, and the decay curves were analyzed by the nonlinear least-squares method. All measurements were repeated at least three times.

Formation of Ceramide by Sphingomyelinase. POPC/C16:0-SM (3:1 molar ratio) LUVs containing either PDCer ($X = 0.01$) or DPH ($X = 0.002$) was made in 5 mM Hepes, 10 mM $CaCl_2$, 2 mM $MgCl_2$, pH 7.4, buffer as described above at a total lipid concentration of 22.5 μM. The substrate LUVs were allowed to equilibrate at 30 °C in the magnetically stirred cuvette for 2 min prior to the initiation of the reaction by the addition of 20 μL of sphingomyelinase solution (10 units/mL) to yield a final enzyme concentration of 0.1 units/mL.

Consequences of the rapid conversion of sphingomyelin to ceramide were monitored spectrophotometrically by measuring changes in the DPH polarization and I_e/I_m for PDCer. The concentrations of Ca^{2+} and Mg^{2+} required for maximal catalytic activity of SMase (*30*) did not affect the fluorescence of the above LUVs (data not shown). As reported by Alonso and co-workers hydrolysis of sphingomyelin containing liposomes by SMase results in their intense aggregation (*30*, *31*). Accordingly, to avoid artifacts in the emission spectra caused by light scattering, we mixed the samples thoroughly prior to fluorescence measurements. At the indicated times 2 mL samples of the reaction mixture were taken and thoroughly mixed by brief (approximately 3 s) vortexing followed by maximal 5 s irradiation in a bath-type sonicator whereafter either fluorescence spectra or polarization was measured as described above. All measurements were repeated at least three times.

To determine the time course of hydrolysis of SM to ceramide, we included ^{14}C-SM ($X = 0.02$, 2 kBq) into POPC/C16:0-SM (0.74:0.23, mole fraction) liposomes. Subsequently, the enzyme reactions were started at 30 °C by the addition of SMase, essentially as described above. The final concentration of lipids was 22.5 μM in 2 mL of 5 mM Hepes, 10 mM $CaCl_2$, 2 mM $MgCl_2$, pH 7.4. At the indicated time points the reactions were stopped by adding 2 mL of

chloroform/methanol (2:1, v/v). The lower organic phase was separated and concentrated by evaporating the solvents whereafter 50 μL of chloroform was added to dissolve the lipids. ^{14}C−SM was separated from the reaction mixture on a TLC plate using chloroform/methanol/water (65:25:4, v/v/v) as a solvent system. The hydrolysis of ^{14}C−SM was quantitated from these TLC plates using a Bio-imaging analyzer BAS-1800 (Fuji Photo Film Co., Tokyo, Japan) connected to a pentium computer for data retrieval and analysis by the dedicated software provided by the instrument manufacturer.

RESULTS

We have recently demonstrated that, when the content of ceramide exceeds $X > 0.1$, this lipid becomes enriched into microdomains, both in the gel state as well as in the liquid crystalline dimyristoylphosphatidylcholine vesicles (*19*). However, this study employed bovine ceramide, with considerable variation in the length of the *N*-acyl chain, from 16 to 27 carbon atoms. The presence of the very long *N*-acyl chains may cause interdigitation similar to that observed in SM membranes (*40, 41*) as well as microdomain formation due to hydrophobic mismatch (*42*). Therefore, to avoid ambiguities in the interpretation of the data caused by the above processes, we carried out similar experiments using the chemically well-defined *N*-palmitoyl-sphingosine (C16:0-Cer) and the corresponding sphingomyelin. Likewise, to be closer to biologically relevant conditions the unsaturated, fluid POPC was used as the matrix instead of DMPC. Pyrene-labeled ceramide analogue, PDCer ($X = 0.01$) was included as a fluorescent reporter. The value for I_e/I_m measured with PDCer in a POPC matrix is roughly the same as for PPDPC in DMPC above T_m, that is, when both lipids are in fluid phase (*19*), indicating the absence of gross lateral segregation of PDCer in POPC (Figure 1).

Effects of C16:0-SM on the Dynamics of POPC Bilayers. PCs and SMs containing similar acyl chains have been shown to be miscible (*21*). This could be confirmed in the present study demonstrating a decrease in I_e/I_m upon increasing X_{SM} in POPC (Figure 1). The reduction in I_e/I_m further implies an ordering effect by C16:0-SM in the binary alloy, in keeping with previous studies (*20, 21*). Increasing membrane order is revealed also by the progressive increase in steady-state polarization *P* for the hydrophobic rodlike fluorophore, DPH, upon increasing X_{SM} (Figure 2). *P* depends on the average angular motion of the fluorophore (*43*). An increase in the membrane free volume V_f allows for more extensive wobbling of the fluorophore, and thus decreases *P* (*44*). Conversely, an increase in this parameter reveals increased membrane order and a reduction in V_f. Steady-state polarization *P* for DPH has been shown to be proportional to its lifetime (e.g., refs *44*, *45*), and Parasassi et al. (*46*) pointed out that changes in DPH lifetime and chain order in membranes are compensatory. However, to exclude the possibility that a decrease in DPH lifetime was causing the increase in *P*, we measured τ as a function of X_{SM}. In brief, our experiments revealed that when X_{SM} in binary POPC/C16:0-SM membranes was increased from 0 to 0.25, τ increased from 7.6 to 8.4 ns, thus confirming the increase in *P* to reflect restricted motion of DPH (Figure 3).

Effects of C16:0-Ceramide on the Dynamics of POPC Bilayers. The above effect of C16:0-SM is in striking contrast to that caused by the corresponding ceramide. More specifically, very little change in I_e/I_m was evident when X_{cer} was increased to 0.05, whereas exceeding this content of C16:0-Cer further, up to $X = 0.25$, caused a progressive, maximally approximately 1.6-fold increase in I_e/I_m (Figure

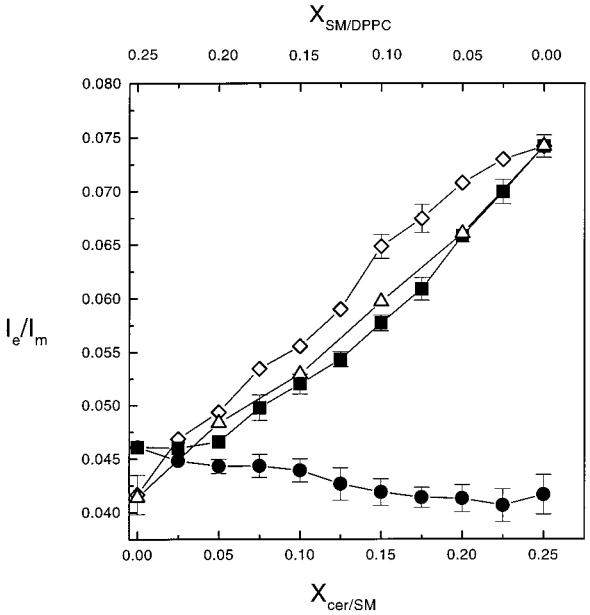

FIGURE 1: Intermolecular I_e/I_m for PDCer ($X = 0.01$) measured for LUVs composed of POPC and the indicated contents of C16:0-ceramide (C16:0-Cer, ■) or C16:0-sphingomyelin (C16:0-SM, ●). Also shown are data for LUVs with a constant total mole fraction of sphingolipids ($X = 0.25$) with varying of the Cer/SM stoichiometry from 0:1 to 1:0 (◇) or substituting SM for the corresponding dipalmitoylphosphatidylcholine, DPPC (△). The upper *x*-axis denotes the mole fraction of either C16:0-sphingomyelin or dipalmitoylphosphatidylcholine for the graphs labeled with open symbols (◇, △). The total lipid concentration was 22.5 μM in 5 mM Hepes, 0.1 mM EDTA, pH 7.4. The temperature was maintained at 30 °C with a circulating waterbath.

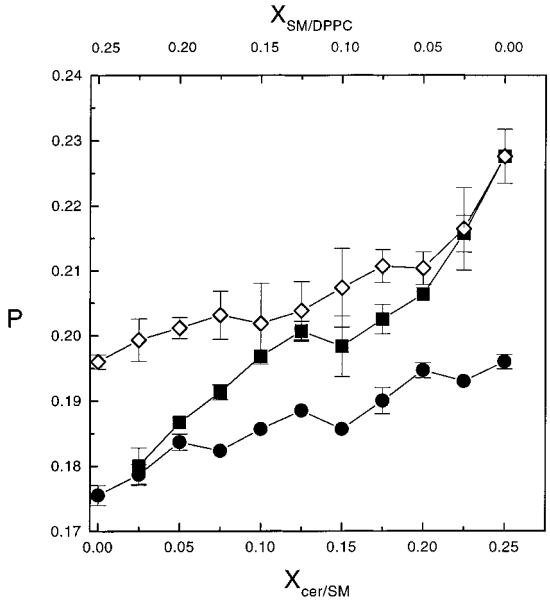

FIGURE 2: Fluorescence polarization *P* for DPH ($X = 0.002$) residing in binary LUVs composed of POPC and C16:0-ceramide (C16:0-Cer, ■), sphingomyelin (C16:0-SM, ●), or varying the stoichiometry of C16:0-ceramide and C16:0-SM similarly as in Figure 1 (◇). Otherwise conditions were as described in the legend for Figure 1.

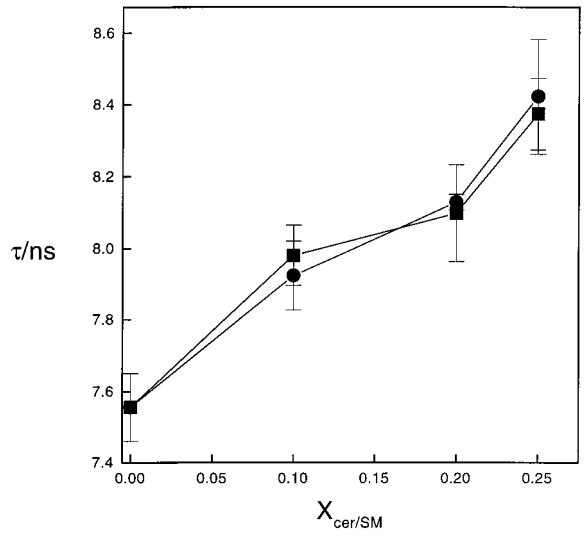

FIGURE 3: Fluorescence lifetime for DPH ($X = 0.002$) in either POPC/C16:0-ceramide (C16:0-Cer, ■) or POPC/C16:0-sphingomyelin (C16:0-SM, ●) binary LUVs. Otherwise conditions were as described in the legend for Figure 1.

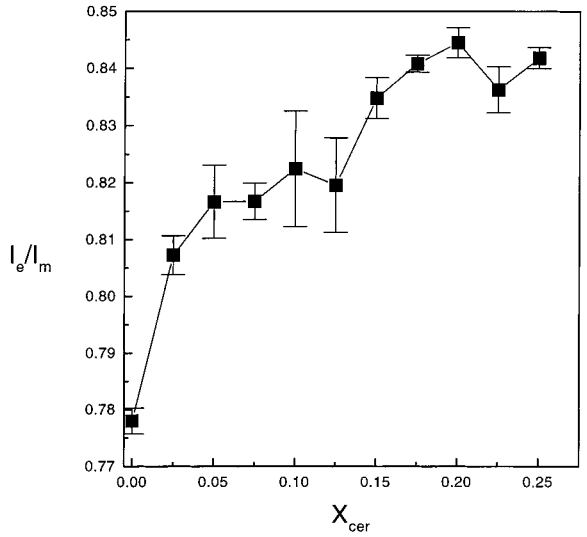

FIGURE 4: Intramolecular I_e/I_m for bisPDPC ($X = 0.001$) in POPC as a function of the content of C16:0-ceramide. The total lipid concentration was 22.5 μM in 5 mM Hepes, 0.1 mM EDTA, pH 7.4. The temperature was maintained at 30 °C.

1). The augmented I_e/I_m could result either from lateral segregation of the probe or from an increased rate of lipid lateral diffusion. To resolve between these two mutually nonexclusive mechanisms, we measured also DPH fluorescence polarization as well as lifetimes (Figure 3). Compared to the effect of C16:0-SM, the increase in DPH polarization due to C16:0-Cer was much more pronounced (Figure 2). The increase in τ was approximately the same as for C16:0-SM/POPC binary membranes. Our previous studies indicated ceramide to reduce membrane free volume, V_f, evident as a reduced wobble angle for DPH (*19*). V_f can be assessed also using the intramolecular excimer forming probe bisPDPC (*47*). When the level of thermal excitation is maintained constant, diminished V_f causes decreased splaying of the two pyrenedecanoyl chains of this probe and thus increases the intramolecular I_e/I_m for this probe (Figure 4). Increased lateral packing density in the bilayer (i.e., decreasing V_f) causes decrement in membrane lateral diffusion (*47*). Accordingly, the increment in lateral diffusion cannot be causing the observed increase in the intermolecular I_e/I_m for PDCer and C16:0-Cer can thus be concluded to be enriched into microdomains.

Tertiary Membranes Composed of C16:0 Ceramide-C16:0-Sphingomyelin/POPC. Given the distinct difference between the effects of C16:0-SM and the corresponding ceramide on POPC bilayers, it was of particular interest to study also tertiary POPC/SM/Cer membranes. These experiments were performed maintaining the total sphingolipid mole fraction ($X_{SM} + X_{cer}$) constant, while varying the molar ratio X_{cer}/X_{SM}. I_e/I_m measured for PDCer at ($X_{SM} + X_{cer}$) = 0.25 and upon increasing X_{cer} from 0 to 0.25 is shown in Figure 1. Notably, compared to the binary Cer/POPC vesicles, the presence of sphingomyelin augmented the increase in I_e/I_m caused by ceramide. A similar experiment measuring DPH polarization revealed increased P in the tertiary membranes (Figure 2). Interestingly, when DPPC was used instead of C16:0-SM (i.e., $X_{DPPC} + X_{cer} = 0.25$ with varying stoichiometry) the values for I_e/I_m for PDCer were close to those measured for the binary POPC/C16:0-Cer liposomes (Figure 1).

Enzymatic Conversion of Sphingomyelin to Ceramide. The above differences in the organization of sphingomyelin and ceramide in a POPC matrix, miscibility, and microdomain formation, respectively, also allowed us to monitor by fluorescence spectroscopy the progress and consequences of the enzymatic conversion of sphingomyelin to ceramide, catalyzed by SMase. To this end, the above experiment performed at a constant mole fraction of sphingolipids and varying Cer/SM stoichiometry can be used for comparison with the enzymatic formation of ceramide. However, although this change in composition to some extent simulates the progress of a SMase-catalyzed reaction, the lipids mixed in an organic solvent are expected to be equally distributed between the inner and outer leaflets of the bilayer. Instead, in the absence of transbilayer rearrangements of the lipids, only sphingomyelin in the outer leaflet of the vesicles should be susceptible to the enzyme.

The time course of enzymatic hydrolysis of SM in POPC/SM (3:1, molar ratio) LUVs was determined by following the loss of radioactivity of ^{14}C-SM by TLC and radioimaging. In keeping with the amount of enzyme used (0.1 international units/mL) the measured hydrolysis of SM was rapid. Of the 11.25 nmol of SM in the substrate LUVs, approximately 85% was converted into ceramide within <3 min, whereafter no further hydrolysis was evident (Figure 5). Importantly, the extent of hydrolysis exceeded 50% of the initial SM in the bilayer, thus indicating rapid rearrangements in the membrane organization to occur in the course of the enzyme reaction. In accordance with the rapid formation of ceramide, also the increase in membrane order (revealed by increment in DPH polarization) was measured on a time scale closely paralleling the extent of degradation of SM (Figure 6). After the rapid increment in P no further changes could be observed.

To obtain further insight into the changes in membrane properties in the course of the SMase reaction, we next monitored the enzyme action under otherwise identical conditions and measuring I_e/I_m for PDCer. Hydrolysis of SM to ceramide in binary POPC/SM (3:1, molar ratio) LUVs by SMase caused first (within ≈10 min) a slight decrease in

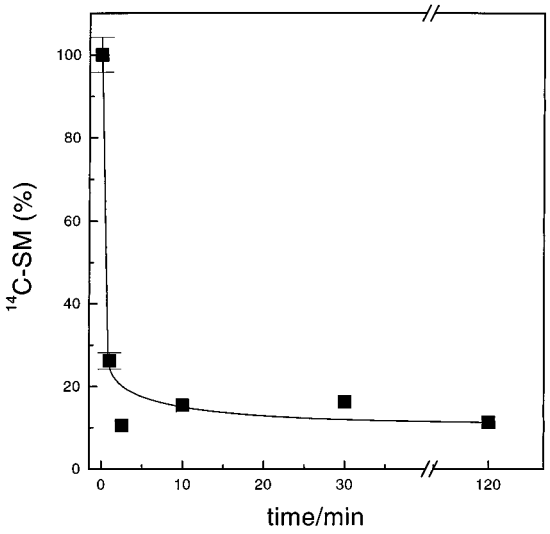

FIGURE 5: The time course for the hydrolysis of ^{14}C-SM in binary POPC/C16:0-SM (3:1) LUVs by SMase (*B. cereus*). The total lipid concentration was 22.5 μM in 5 mM Hepes, 10 mM $CaCl_2$, 2 mM $MgCl_2$, pH 7.4, and the enzyme concentration was 0.1 units/mL. The temperature was maintained at 30 °C. The solid line represents a guide to the eye.

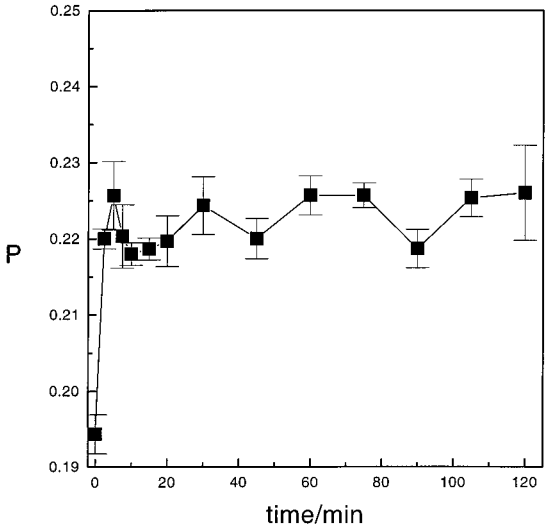

FIGURE 6: The time course for changes in fluorescence polarization (P) for DPH ($X = 0.002$) residing in POPC/C16:0-SM LUVs (3:1) after the addition of SMase (*B. cereus*, final concentration 0.1 units/mL). The total lipid concentration was 22.5 μM in 5 mM Hepes, 10 mM $CaCl_2$, 2 mM $MgCl_2$, pH 7.4. The temperature was maintained at 30 °C with a circulating waterbath.

I_e/I_m (Figure 7). This transient decrement was followed by a nearly linear increase in I_e/I_m with times, until at 105 min an apparent steady state was reached, with no further changes in 3 h, the longest period measured. To elucidate the mechanism(s) limiting the rate of microdomain formation, we increased the lateral diffusion of the membrane lipids by a rapid, transient heating of the reaction mixture after the formation of C16:0-Cer was complete (Figure 5). More specifically, 2.5 min after the addition of SMase the samples were maintained briefly (for 2 min) at 65 °C and then cooled back to 30 °C for the measurement of I_e/I_m. Notably, this brief, transient exposure of the sample to a higher thermal excitation caused the steady state in I_e/I_m to be reached significantly faster, in ≈60 min. These data suggest that, following the rapid conversion of SM to ceramide, the

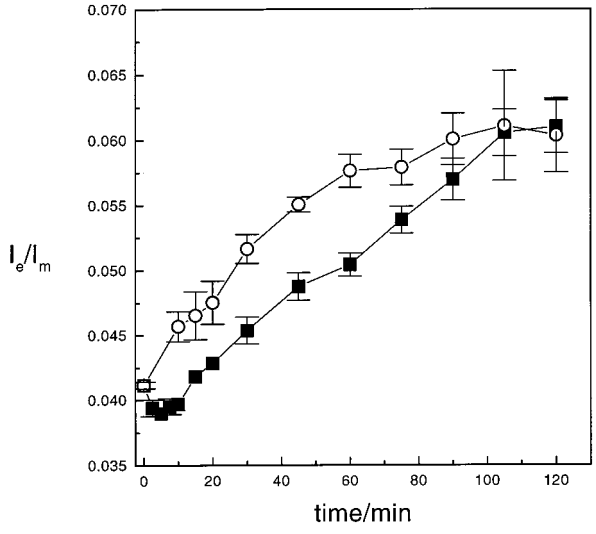

FIGURE 7: The time course of changes in I_e/I_m for PDCer ($X = 0.01$) in POPC/C16:0-SM (3:1, molar ratio) LUVs upon the hydrolytic action of SMase (*B. cereus*). Two sets of data are illustrated, as follows. In one experiment the enzyme was added at 30 °C whereafter the reaction was allowed to proceed at this temperature for the indicated period of time (■). In the other experiment (○) the reaction was allowed to proceed for 2.5 min at 30 °C whereafter the reaction mixture was maintained at 65 °C for 2 min. Subsequently, the sample was cooled to 30 °C and processed identically to the control maintained at 30 °C (■). The enzyme reactions were initiated by the addition of SMase (final concentration 0.1 units/mL) whereafter fluorescence spectra were recorded at the given times as described under Experimental Procedures. The total lipid concentration was 22.5 μM in 2 mL of 5 mM Hepes, 10 mM $CaCl_2$, 2 mM $MgCl_2$, pH 7.4.

organization of the membrane no longer corresponds to thermodynamic equilibrium but the membrane is in a metastable state. Subsequently, the latter slowly decays to a new steady state, the rate of the reorganization process being diffusion-controlled and limited by the highly viscous state of the bilayer.

DISCUSSION

Current studies on ceramide-mediated signaling cascades are focused on the search for its downstream effectors. When considering the mechanism(s) of action of ceramide, it is essential to emphasize that it is an amphipathic molecule and thus strongly favors partitioning into bilayers. Therefore, an understanding of the properties of ceramide-containing membranes is needed to elucidate the roles of lipid−lipid and lipid−protein interactions in determining the biological activities of this lipid. To this end, Arora et al. (*48*) presented evidence for hepatocyte cell death being caused by the intrinsic properties of ceramide, the exact mechanism(s) remaining unresolved.

The precursor for ceramide is sphingomyelin, an ubiquitous and abundant phospholipid of eukaryote cells. The significance of this lipid to the structure and function of membranes remains unknown. The total membrane content of PC and SM has been proposed to be constant, whereas the molar ratios of these two lipids seem to vary with the state of the cell (*49*). It was suggested that, by changing the molar ratios, the acyl chain ordering could be controlled without altering other structural features of the bilayer (*21*). In keeping with previous studies on mixed SM/PC membranes (*20*, *23*), we could confirm in the present study that

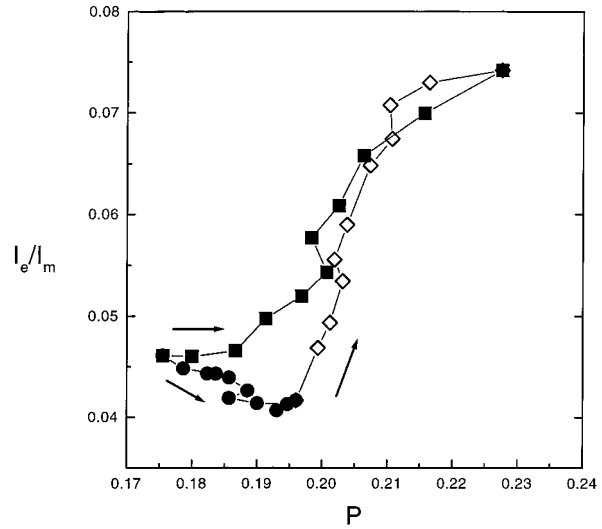

FIGURE 8: Fluorescence polarization (*P*) for membrane-incorporated DPH as a function of I_e/I_m for PDCer in binary LUVs composed of POPC and C16:0-ceramide (C16:0-Cer, ■), sphingomyelin (C16:0-SM, ●), or varying the stoichiometry of C16:0-ceramide and C16:0-SM similarly as in Figure 1 (◇). The arrow depicts the direction of increasing X_{cer} or X_{SM}. The data are taken from measurements shown in Figures 1 and 2.

C16:0-SM is miscible with POPC. Likewise, increasing the mole fraction of C16:0-SM causes an augmented membrane order revealed by an increase in *P* (Figure 2), with a concomitant decrement in lateral diffusion, evident as diminished I_e/I_m (Figure 1). Upon increasing X_{SM}, an almost linear reciprocal relationship between these two parameters is observed (Figures 1, 8).

Our previous studies on natural ceramide with large differences in the lengths of the *N*-acyl chains provided evidence for the formation of microdomains enriched in this lipid (*19*). The present results clearly reveal microdomain formation also in POPC/C16:0-Cer LUVs and demonstrate that the long *N*-acyl chains are not required. In brief, an increase in *P* upon increasing X_{cer} is accompanied with decreasing lateral diffusion which should decrease I_e/I_m for PDCer. However, the opposite is observed, thus indicating lateral enrichment of the pyrene-labeled lipid. Comparison of DPH polarization and I_e/I_m for PDCer shows that when $X_{cer} \rightarrow 0.05$, *P* increases while I_e/I_m is only moderately affected (Figures 1,2, and 8). Thereafter, exceeding this content of ceramide, a distinct increase in I_e/I_m is evident, indicating local enrichment of the probe (Figure 8). The concentration of C16:0-Cer needed for microdomain formation is thus somewhat less than for the natural ceramide for which $X = 0.075$ is required (*19*). Although our earlier studies were performed with a DMPC matrix, this difference is likely to reflect the long *N*-acyl chains of natural ceramides perturbing the membrane packing more than those of C16:0-Cer, so as to impede ceramide−ceramide interactions. In conclusion, our data thus show microdomain formation to arise due to the properties of the headgroup of ceramide and exclude hydrophobic mismatch as the mechanism causing lateral segregation of this lipid. Although no definitive mechanism can be pointed at this stage, when taking into account the chemical structure of ceramide, a feasible explanation could be hydrogen bonding. Compared to glycerophospholipids which can act only as acceptors of hydrogen bonds, sphingolipids such as SM and Cer can act as both acceptors and donors by their hydroxyl and amino groups, respectively, as well as due to the phosphate moiety of the former lipid (*27*). To this end, also the mechanism preventing domain formation by SM is of interest. One possibility is provided by the large hydration shell of the phosphocholine group causing a strong steric hindrance prohibiting hydrogen bonding in sphingomyelin−sphingomyelin interactions.

The mechanism(s) causing increase in I_e/I_m for PDCer upon increasing X_{cer} is (are) of interest. If PDCer would reside within the ceramide-enriched domains, an increase in X_{cer} would dilute PDCer and thus decrease I_e/I_m. This is not observed. On the other hand, preferential partitioning of PDCer into POPC domains would increase I_e/I_m as X_{POPC} decreases. However, increments of I_e/I_m by this mechanism can readily be estimated to be negligible. To this end, packing of the saturated ceramide in microdomains can be anticipated to be tight. Due to its bulky pyrene moiety the lack of alloying of PDCer into the C16:0-Cer-enriched domains is not unexpected. Accordingly, the perhaps most feasible explanation is that PDCer becomes enriched into the boundaries of domains enriched in ceramide (*50*).

These data also allow us to discuss the composition of the domains enriched in POPC in the binary membrane. Below $X_{cer} = 0.05$ ceramide-enriched microdomains are not observed. Accordingly, we can assume that ceramide is dispersed in the membrane and thus affects the entire bilayer. Yet, exceeding $X_{cer} = 0.05$ causes ceramide molecules to become enriched into microdomains, thus limiting further effects on the POPC matrix. Because of its two bulky pyrene moieties, bisPDPC can be readily expected to be expelled from the tightly packed ceramide-enriched microdomains. This would explain why only a relatively small increase in I_e/I_m for bisPDPC is observed (Figure 4).

To be able to interpret experiments in which ceramide is formed from SM by the hydrolytic action of SMase, we first studied tertiary membranes composed of POPC, C16:0-SM, and C16:0-Cer. Notably, when the mole fraction of sphingolipids is maintained constant ($X = 0.25$) and the SM/ceramide stoichiometry is varied from 1:0 and 0:1, the presence of SM augments the formation of ceramide-enriched microdomains evident as enhanced I_e/I_m for PDCer (Figure 1). These data also show that the correlation between *P* and I_e/I_m is not trivial except in the case of POPC/C16:0-SM, where increased membrane order is accompanied with a decrease in I_e/I_m. However, the correlation between *P* and I_e/I_m in binary POPC/C16:0-Cer and in tertiary membranes clearly supports increments of I_e/I_m to be caused by an enrichment of PDCer into microdomains, that is, into the phase boundaries. Interestingly, gradual replacement of Cer with SM (up to $X_{cer} = 0.20$) in tertiary membranes has a rather minor effect on acyl chain order (Figure 8). Instead, the enrichment of PDCer is significantly enhanced. In contrast, substituting C16:0-SM by DPPC, the corresponding PC, in these tertiary membranes does not result in an enhanced I_e/I_m (Figure 1). This indicates a specific interaction between SM and ceramide, probably caused by hydrogen bonding between amino and hydroxyl groups of these lipids.

In the next series of experiments we investigated the consequences of enzymatic conversion of SM to ceramide, catalyzed by sphingomyelinase. A sufficient amount of enzyme was used so as to ensure rapid completion of the

reaction, confirmed by the decrease of ^{14}C-radioactivity in SM (Figure 5). Assuming SM in these vesicles to be initially approximately equally distributed between the inner and outer leaflets of the bilayer, one would anticipate about 50% of the total SM to be hydrolyzed to ceramide. Intriguingly, our data show that approximately 85% of SM was degraded within <3 min of the reaction whereafter no further loss of SM was evident. This is somewhat unexpected as previous studies have shown approximately 40% of SM in SM/eggPE/cholesterol (2:1:1 molar ratio) LUVs to be hydrolyzed by SMase (*30*, *31*). This difference could be caused by cholesterol. Studies addressing this issue are currently in progress in our laboratory.

The defects generated upon the conversion of sphingomyelin to ceramide could be severe enough to allow passage of the enzyme into the LUVs. However, in this case complete hydrolysis of SM should occur. As this is not observed, the former mechanism is perhaps more feasible. Interestingly, the flip-flop rate for a rather similar molecule, diacylglycerol, has been estimated to be in the range of milliseconds (*51*). It has been shown that the action of SMase on SM-containing vesicles causes leakage of their contents, indicating some kind of defects to be generated (*30*, *31*). Such defects together with the differences in the lateral packing of the inner and outer leaflets could readily promote the transfer of SM into the outer leaflet.

Sphingomyelinase has been shown to promote the aggregation of sphingomyelin-containing vesicles, suggested to be caused by the accumulated ceramide (*30*). This could be confirmed in the present study. In contrast, ceramide-containing (up to $X_{cer} = 0.25$) LUVs formed by lipid mixing in organic solvent did not show any signs of aggregation for up to 24 h of incubation. The aggregation of LUVs due to the action of SMase could result from the initially asymmetric production of ceramide in the outer leaflet of the vesicles or by the enzyme protein itself. In both alternatives the actual mechanism(s) remain(s) open at this stage.

The physical (phase) state of the membrane has been proposed to be directly involved in the activation of a wide variety of proteins (*52*, *53*). Likewise, phase separation and domain formation in biomembranes have been postulated to be of functional significance (*32*). Peripheral interactions of proteins such as protein kinase C with membrane surfaces can be modulated by the lateral distribution of phospholipids (*54*) and the physical properties of the membrane (*55*). Hinderliter et al. (*56*) demonstrated that diacylglycerol-enriched domains were necessary for the maximal activity of this enzyme. Local dynamic fluctuations and domain boundaries might play a role in enzyme activation and/or attachment of proteins to the plasma membrane, as suggested for phospholipase A_2 (*57*). The formation of ceramide in the plasma membrane following ligand binding has been shown in a number of studies (e.g., ref *17*) and could be relevant in the activation of the high-affinity receptor for IgE on mast cells and basophils (FcϵRI), for instance (*58*). We demonstrate in the present study that the hydrolysis of SM to ceramide results in microdomain formation. Importantly, although the formation of ceramide is rapid, changes in the lateral reorganization in response to the change in the chemical composition require significantly longer time. Whether this is also the case in the plasma membrane of living cells requires further studies. Formation of ceramide-enriched membrane domains could be relevant in the downstream signal transduction by this lipid, sequestering specific proteins into domains such as caveolae.

ACKNOWLEDGMENT

We thank M. Sc. Arimatti Jutila for help with the fluorescence lifetime measurements, Birgitta Rantala and Outi Tamminen for skillful technical assistance, and members of our group for rewarding discussions.

REFERENCES

1. Chao, M. V. (1995) *Mol. Cell. Neurosci. 6*, 91−96.
2. Hannun, Y. A. (1994) *J. Biol. Chem. 269*, 3125−3128.
3. Hannun, Y. A. (1996) *Science 274*, 1855−1859.
4. Obeid, L. M., and Hannun, Y. A. (1995) *J. Cell. Biochem. 58*, 191−198.
5. Pushkareva, M., Obeid, L. M., and Hannun, Y. A. (1995) *Immunol. Today 16*, 294−297.
6. Saba, J. D., Obeid, L. M., and Hannun, Y. A. (1996) *Philos. Trans. R. Soc. London, Ser. B. 351*, 233−241.
7. Spiegel, S., Foster, D., and Kolesnick, R. N. (1996) *Curr. Opin. Cell Biol. 8*, 159−167.
8. Davis, R. J. (1993) *J. Biol. Chem. 268*, 14553−14556.
9. Hannun, Y. A., and Obeid, L. M. (1995) *Trends Biochem. Sci. 20*, 73−77.
10. Kolesnick, R. N., and Golde, D. W. (1994) *Cell 77*, 325−328.
11. Kruth, H. S. (1997) *Curr. Opin. Lipidol. 8*, 246−252.
12. Schurer, N. Y., and Elias, P. M. (1991) *Adv. Lipid Res. 24*, 27−56.
13. Elias, P. M., and Menon, G. K. (1991) *Adv. Lipid Res. 23*, 753−758.
14. Geilen, C. C., Wieder, T., and Orfanos, C. E. (1997) *Arch. Dermatol. Res. 289*, 559−566.
15. Jarvis, W. D., Grant, S., and Kolesnick, R. N. (1996) *Clin. Cancer Res. 2*, 1−6.
16. Tomita, M., Ueda, Y., Tamura, H., Taguchi, R., and Ikezava, H. (1991) *Biochim. Biophys. Acta 1203*, 85−92.
17. Liu, P., and Anderson, G. W. (1995) *J. Biol. Chem. 270*, 27179−27185.
18. Lisanti, M. P., Scherer, P. E., Tang, Z., and Sargiacomo, M. (1994) *Trends Cell Biol. 4*, 231−235.
19. Holopainen, J. M., Lehtonen, J. Y. A., and Kinnunen, P. K. J. (1997) *Chem. Phys. Lipids 88*, 1−13.
20. Calhoun, W. I., and Shipley, G. G. (1979) *Biochemistry 18*, 1717−1722.
21. Lentz, B. R., Hoechli, M., and Barenholz, Y. (1981) *Biochemistry 20*, 6803−6809.
22. Shipley, G. G., Avecilla, L. S., and Small, D. M. (1974) *J. Lipid Res. 15*, 124−131.
23. McKeone, B. J., Pownall, H. J., and Massey, J. B. (1986) *Biochemistry 25*, 7711−7716.
24. Nieva, J. L., Bron, R., Corver, J., and Wilschut, J. (1994) *EMBO J. 13*, 2797−2804.
25. Jwa Hidari, K. I.-P., Ichikawa, S., Fujita, T., Sakiyama, H., and Hirabayashi, Y. (1997) *J. Biol. Chem. 271*, 14636−14641.
26. Merrill, A. H., Jr., and Jones, D. D. (1990) *Biochim. Biophys. Acta 1044*, 1−12.
27. Shah, J., Atienza, J. M., Duclos, R. I., Jr., Rawlings, A. V., Dong, Z., and Shipley, G. G. (1995) *J. Lipid Res. 36*, 1936−1944.
28. Shah, J., Atienza, J. M., Rawlings, A. V., and Shipley, G. G. (1995) *J. Lipid Res. 36*, 1945−1955.
29. Huang, H.-W., Goldberg, E. M., and Zidovetski, R. (1996) *Biochem. Biophys. Res. Commun. 220*, 834−838.
30. Ruiz-Argüello, M. B., Basáñez, G., Goñi, F. M., and Alonso, A. (1996) *J. Biol. Chem. 271*, 26616−26621.
31. Basáñez, G., Ruiz-Argüello, M. B., Alonso, A., Goñi, F. M., Karlsson, G., and Edwards, K. (1997) *Biophys. J. 72*, 2630−2637.

32. Kinnunen, P. K. J. (1991) *Chem. Phys. Lipids 57*, 375−399.
33. Mouritsen, O. G., and Kinnunen, P. K. J (1996) in *Biological Membranes* (Merz, K., Jr., and Roux, B., Eds.) pp 463−502, Birkhäuser, Boston, MA.
34. Lapidot, Y., Rappoport, S., and Wolman, Y. (1967) *J. Lipid Res. 8*, 142−145.
35. Ong, D. E., and Brady, R. N. (1972) *J. Lipid Res. 13*, 818−822.
36. MacDonald, R. C., MacDonald, R. I., Menco, B. M., Takeshita, K., Subbarao, N. K., and Hu, L. R. (1991) *Biochim. Biophys. Acta 1061*, 297−303.
37. Kinnunen, P. K. J., Tulkki, A.-P., Lemmetyinen, H., Paakkola, J., and Virtanen, J. A. (1987) *Chem. Phys. Lett. 136*, 539−545.
38. Kinnunen, P. K. J., Kõiv, A., and Mustonen, P. (1993) in *Fluorescence Spectroscopy* (Wolfbeis, O. S., Ed.) pp 159−169, Springer-Verlag, Berlin, Germany.
39. Duportail, G., and Lianos, P. (1996) in *Vesicles* (Rosoff, M., Ed.) pp 295−372, Marcel Decker, New York.
40. Levin, I. W., Thompson, T. E., Barenholz, Y., and Huang, C. (1985) *Biochemistry 24*, 6282−6286.
41. Maulik, P. R., Atkinson, D., and Shipley, G. G. (1986) *Biophys. J. 50*, 1071−1077.
42. Lehtonen, J. Y. A., Holopainen, J. M., and Kinnunen, P. K. J. (1996) *Biophys. J. 70*, 1753−1760.
43. Lakowicz, J. R. (1983) Fluorescence polarization, in *Principles of Fluorescence Spectroscopy*, pp 111−151, Plenum, New York.
44. Chong, P. L.-G., Cossins, A. R., and Weber, G. (1983) *Biochemistry 22*, 409−415.
45. Chong, P. L.-G., and Weber, G. (1983) *Biochemistry 22*, 5544−5550.
46. Parasassi, T., De Stasio, G., Rusch, R. M., and Gratton, E. (1991) *Biophys. J. 59*, 466−475.
47. Lehtonen, J. Y. A., and Kinnunen, P. K. J. (1994) *Biophys. J. 66*, 1981−1990.
48. Arora, A. S., Jones, B. J., Patel, T. C., Bronk, S. F., and Gores, G. J. (1997) *Hepatology 25*, 958−963.
49. Barenholz, Y., and Thompson, T. E. (1980) *Biochim. Biophys. Acta 604*, 129−158.
50. Jutila, A., and Kinnunen, P. K. J. (1997*) J. Phys. Chem. B 101*, 7635−7640.
51. Hamilton, J. A., Bhamidipati, S. P., Kodali, D. R., and Small, D. M. (1991) *J. Biol. Chem. 266*, 1177−1186.
52. Kinnunen, P. K. J. (1996) in *Handbook of Nonmedical Applications of Liposomes* (Lasic, D. D., and Barenholz, Y., Eds.) pp 153−171, CRC Press, Inc., Boca Raton, FL.
53. Kinnunen, P. K. J. (1996) *Chem. Phys. Lipids 81*, 151−166.
54. Dibble, A. R. G., Hinderliter, A. K., Sando, J. J., and Biltonen, R. L. (1996) *Biophys. J. 71*, 1877−1890.
55. Goldberg, E. M., and Zidovetski, R. (1997) *Biophys. J. 73*, 2603−2614.
56. Hinderliter, A. K., Dibble, A. R. G., Biltonen, R. L., and Sando, J. J. (1997) *Biochemistry 36*, 6141−6148.
57. Hønger, T., Jörgensen, K., Biltonen, R. L., and Mouritsen, O. G. (1996) *Biochemistry 35*, 9003−9006.
58. Field, K. A., Holowka, D., and Baird, B. (1997) in *Signal Transduction in Mast Cells and Basophils* (Razin, E., Pecht, I., and Rivera, J., Eds.) (in press).

BI980915E